

# **PS Investigation of Petrophysical-Property Heterogeneity for Electrofacies Classification in Carbonate Reservoirs\***

**Fnu Suriamin<sup>1</sup> and Matthew J. Pranter<sup>1</sup>**

Search and Discovery Article #41906 (2016)\*\*

Posted October 31, 2016

\*Adapted from poster presentation given at AAPG 2016 Annual Convention and Exhibition, Calgary, Alberta, Canada, June 19-22, 2016

\*\*Datapages © 2016 Serial rights given by author. For all other rights contact author directly.

<sup>1</sup>University of Oklahoma, Norman, Oklahoma, United States ([fnu.suriamin-1@ou.edu](mailto:fnu.suriamin-1@ou.edu))

## **Abstract**

Electrofacies classification for rock typing in complex carbonate reservoirs is very challenging due to high degrees of heterogeneity in lithology, mineralogy, and pore structure. In extreme cases, multivariate pattern recognition and classification methods such as discriminant function analysis, principal component analysis, and cluster analysis using conventional well logs are insufficient for electrofacies classification, particularly in carbonate reservoirs with “low dynamic” log curves. This study investigates how heterogeneity of petrophysical properties can improve electrofacies classification for rock typing in carbonate reservoirs. It utilizes statistical measures of heterogeneity, Lorentz Coefficient, to quantify variability in petrophysical properties. Within this investigation, the Heterogeneity Logs based on wireline-log data including the gamma-ray, density, neutron, sonic, and photoelectric-factor log suite are calculated over set intervals of 10 m, 5 m, 3 m, and 2 m (33 ft, 17 ft, 10 ft, 7 ft) through Mississippian limestones of the Mid-continent. The investigation of Heterogeneity Logs shows a relationship between Heterogeneity Logs with geological features; for example, the lithofacies 6, the thick-bedded peloidal packstone-grainstone, shows relatively increasing Heterogeneity Log NPHI values. This relationship leads to consideration of using Heterogeneity Logs for fluid-flow zone characterization. The Heterogeneity Logs and other predictor variables from well-log data are selected and linked to core lithofacies to train Artificial-neural-network (ANN), Self-organizing-map (SOM), and Multi-resolution Graph-based Clustering (MRGC) models for predicting lithofacies in wells without core. Finally, the results are compared with the widely used ANN clustering technique which utilizes only the five predictor variables logs including gamma ray, deep resistivity, photoelectric effect, difference between neutron porosity and density porosity, and average of neutron porosity and density porosity.

## **References Cited**

Birch, C.B., 2015, Reservoir-scale stratigraphy, sedimentology, and porosity characteristics of Mississippian reservoirs, northeastern Anadarko Shelf, Oklahoma: Master's thesis, University of Oklahoma, Norman, Oklahoma. 81 p.

Campbell, J.A., C.J. Mankin, A.B. Schwarzkopf, and J.J. Raymer, 1988, Habitat of petroleum in Permian rocks of the midcontinent region: in, Permian Rocks of the Midcontinent, W.A. Morgan and J.A. Babcock, eds.: Midcontinent Society of Economic Paleontologists and

Mineralogists, Special Publication No. 1, p. 13-35.

Dutton, S.P., 1984, Fan-Delta Granite Wash of the Texas Panhandle: Oklahoma City Geological Society, vol. Short Course Notes, p. 1-44.  
Fitch, P., S. Davies, M. Lovell, T. Pritchard, and C. Sirju, 2010, Heterogeneity In Carbonate Petrophysical Properties: Application to Fluid Flow Units And Sampling Strategies: SPWLA 51st Annual Logging Symposium, Perth, Australia, Society of Petrophysicists and Well-Log Analysts.

Johnson, K.S. and K.V. Luza, 2008, Earth sciences and mineral resources of Oklahoma: Educational Publication 9, Oklahoma Geological Survey, 22 p.

LoCricchio, E., 2012, Wash Play Overview, Anadarko Basin: Stratigraphic Framework and Controls on Pennsylvanian Granite Wash Production, Anadarko Basin, Texas and Oklahoma: AAPG Search and Discovery Article, no. 110163, web accessed September 25, 2016, [http://www.searchanddiscovery.com/documents/2012/110163locricchio/ndx\\_locricchio.pdf](http://www.searchanddiscovery.com/documents/2012/110163locricchio/ndx_locricchio.pdf).

McConnell, D.A., 1989, Determination of Offset across the Northern Margin of the Wichita Uplift, Southwest Oklahoma: Geological Society of America Bulletin, v. 101, p. 1317-1332.

Mazzullo, S.J., 2011, Mississippian oil reservoirs in the southern midcontinent: New exploration concepts for a mature reservoir objective: Search and Discovery Article 10373, web accessed September 25, 2016, [http://www.searchanddiscovery.com/pdfz/documents/2011/10373mazzullo/ndx\\_mazzullo.pdf.html](http://www.searchanddiscovery.com/pdfz/documents/2011/10373mazzullo/ndx_mazzullo.pdf.html).

Nissen, S.E., K.J. Marfurt, and T.R. Carr, 2004, Identifying subtle fracture trends in the Mississippian saline aquifer unit using new 3-D seismic attributes: Kansas Geological Survey Open File Report, no. 56.

Northcutt, R.A. and J.A. Campbell, 1995, Geologic provinces of Oklahoma: Oklahoma Geological Survey Open-File Report 5-95, 1 sheet, scale 1:750,000, 6-page explanation and bibliography.



# 6. Core Lithofacies

## Devon Energy 1-7 SWD Frieouf

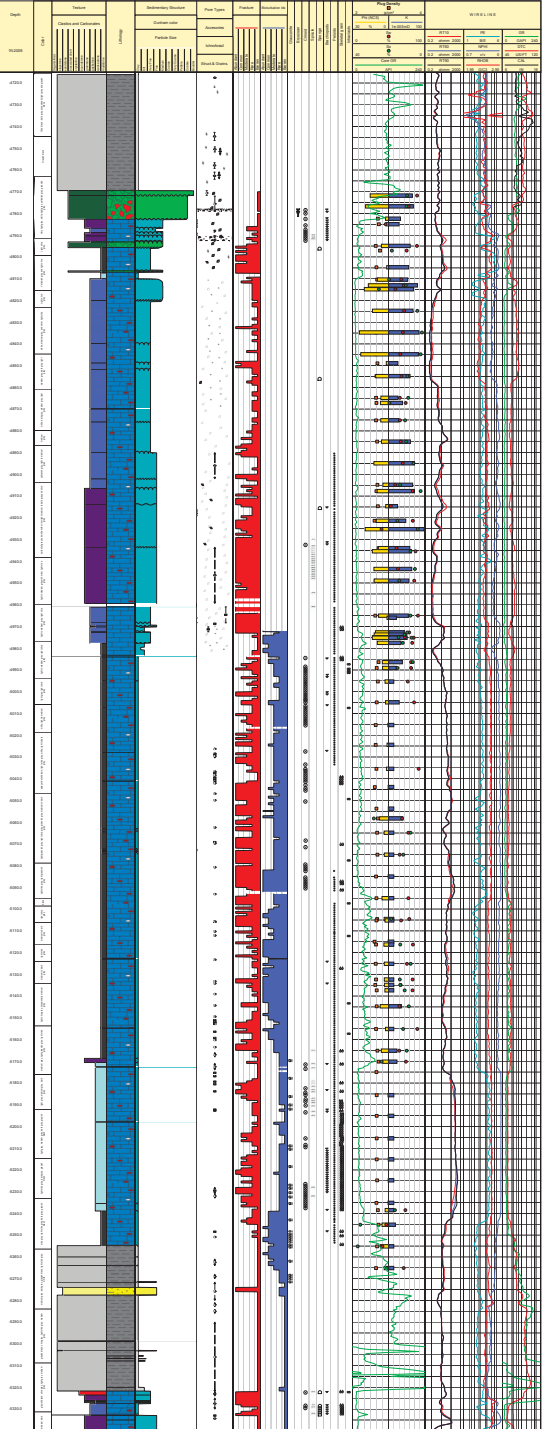


Figure 9. Core description of well Devon Energy 1-7 SWD Frieouf, one of the key cores that is located in the northernmost of the study area. Seven (7) lithofacies classes are observed based on detailed core description in the Mid-continent Mississippian Limestone including: 1. brecciated chert; 2. skeletal packstone-grainstone; 3. peloidal mudstone-wackestone; 4. bioturbated peloidal packstone-grainstone; 5. nodular peloidal packstone-grainstone; 6. bedded peloidal packstone-grainstone; and 7. bioturbated mudstone-wackestone. Examples of each lithofacies characteristics are depicted in the core and thin section images. Typical well-log responses of each lithofacies are shown on the right tracks; including Gamma Ray (GR), Resistivity (RT10, RT60, RT90), Bulk Density (RHOB), Neutron porosity (NPHI), photoelectric effect (PE), and Compressional Sonic travel time log (DTC). Several wells have Spectral Gamma Ray and Nuclear Magnetic Resonance. Routine-core-analysis data including porosity, permeability, grain density, and fluid saturation of selected depths are also plotted. Note that most porosity measurements in the bioturbated mudstone-wackestone are extremely low. This core penetrated the Woodford Shale and Hunton carbonates.

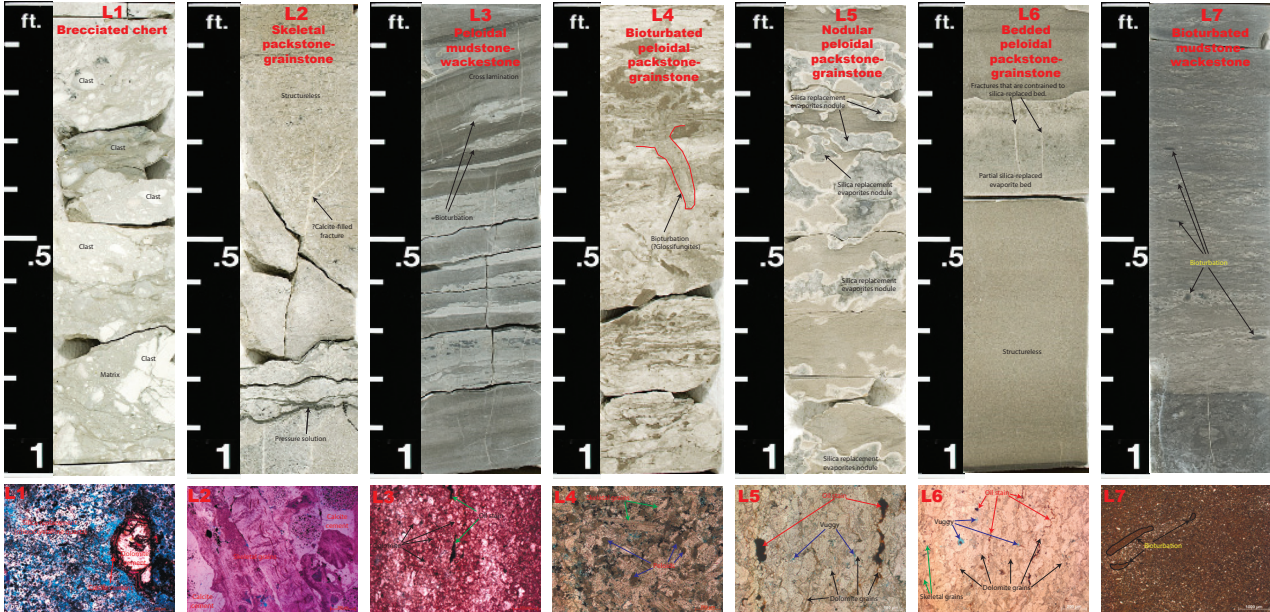


Figure 10. Core photos and thin section photomicrographs for each lithofacies observed in Devon Energy 1-7 SWD Frieouf: L1. brecciated chert, note that most of the clasts are cherts with both matrix-supported and grain-supported textures; L2. skeletal packstone-grainstone, note that this facies is structureless with common pressure solution filled fractures; L3. peloidal mudstone-wackestone, note the cross lamination and compacted bioturbation; L4. bioturbated peloidal packstone-grainstone, note the original texture is destroyed by bioturbation and possibly glossifungites ichnofacies, whitish areas are silica replacement. L5. nodular peloidal packstone-grainstone, note that nodules are irregular (convolute) in shape and show white rind with dark gray center. Silica-replaced evaporites exhibit laterally coalescing nodules that form horizontal anastomosing beds, organic-matter wisps exist between and drape them; L6. bedded peloidal packstone-grainstone, note the very light gray bed consists of silica-replaced evaporites and fractures are constrained to the bed. L7. bioturbated mudstone-wackestone, note the original texture is completely destroyed by bioturbation.

# 7. Statistical Data Analysis

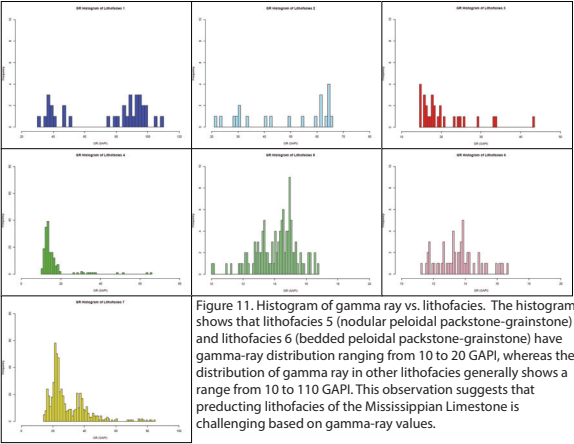


Figure 11. Histogram of gamma ray vs. lithofacies. The histogram shows that lithofacies 5 (nodular peloidal packstone-grainstone) and lithofacies 6 (bedded peloidal packstone-grainstone) have gamma-ray distribution ranging from 10 to 20 GAPI, whereas the distribution of gamma ray in other lithofacies generally shows a range from 10 to 110 GAPI. This observation suggests that predicting lithofacies of the Mississippian Limestone is challenging based on gamma-ray values.

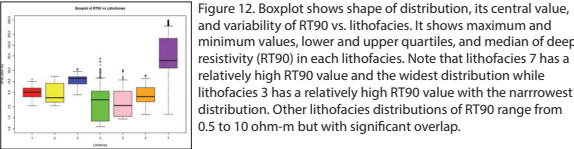


Figure 12. Boxplot shows shape of distribution, its central value, and variability of RT90 vs. lithofacies. It shows maximum and minimum values, lower and upper quartiles, and median of deep resistivity (RT90) in each lithofacies. Note that lithofacies 7 has a relatively high RT90 value and the widest distribution while lithofacies 3 has a relatively high RT90 value with the narrowest distribution. Other lithofacies distributions of RT90 range from 0.5 to 10 ohm-m but with significant overlap.

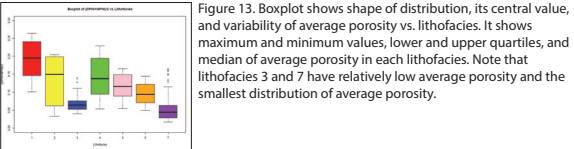


Figure 13. Boxplot shows shape of distribution, its central value, and variability of average porosity vs. lithofacies. It shows maximum and minimum values, lower and upper quartiles, and median of average porosity in each lithofacies. Note that lithofacies 3 and 7 have relatively low average porosity and the smallest distribution of average porosity.

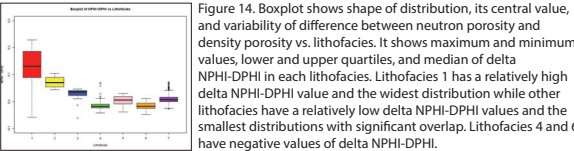


Figure 14. Boxplot shows shape of distribution, its central value, and variability of difference between neutron porosity and density porosity vs. lithofacies. It shows maximum and minimum values, lower and upper quartiles, and median of delta NPHI-DPHI in each lithofacies. Lithofacies 1 has a relatively high delta NPHI-DPHI value and the widest distribution while other lithofacies have a relatively low delta NPHI-DPHI values and the smallest distributions with significant overlap. Lithofacies 4 and 6 have negative values of delta NPHI-DPHI.

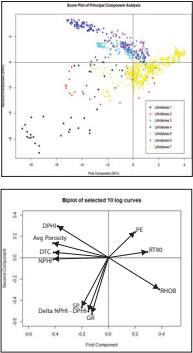


Figure 15. Score plot of principal component analysis. On first component, lithofacies 4, 5, and 6 show similar directions and are therefore challenging to be separated. However the three (lithofacies) may be separated from lithofacies 7 which has a different direction. It is difficult to separate lithofacies 1, 2, and 3 either on first or second component.

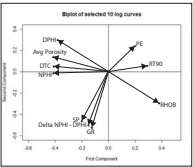


Figure 16. Biplot of principal component analysis. On first component, training data can be separated by porosity data (NPHI, DPHI, and Avg Porosity), sonic log, photoelectric effect (PE), and deep resistivity (RT90). On second component, gamma ray (GR), spontaneous potential (SP), and difference between neutron porosity and density porosity (Delta NPHI-DPHI) have a similar response direction.

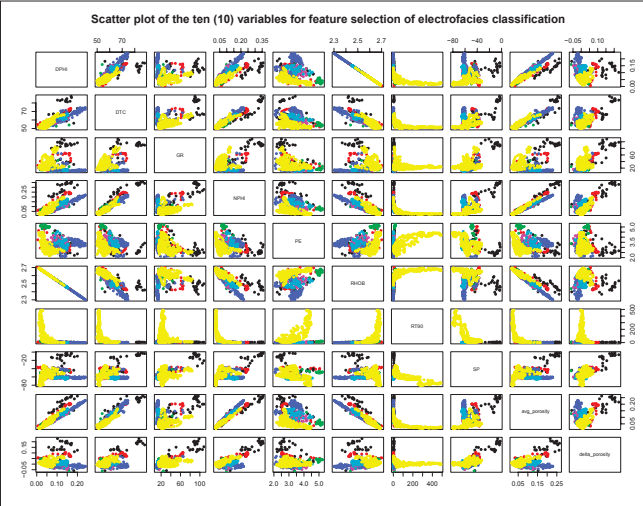


Figure 17. Pairwise scatter plot of ten (10) variables for feature selection of electrofacies classification. The plots are color-coded by electrofacies. Most, if not all, training data show significant overlap and are challenging to separate using basic statistical analysis as well as principal-component analysis.

8. Heterogeneity Logs

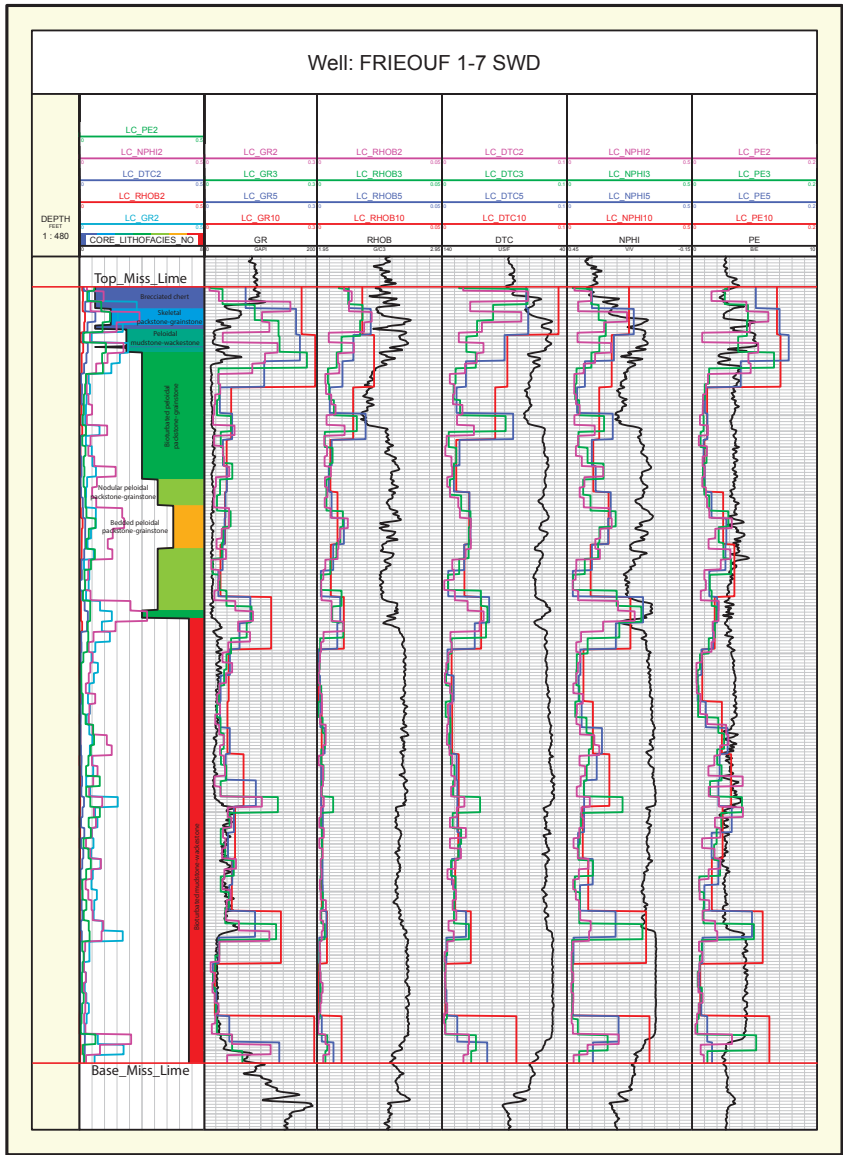


Figure 18. The Lorenz Coefficient Heterogeneity Logs for the Mid-continent Mississippian Limestone interval of well Frieouf 1-7 SWD based on 10-m, 5-m, 3-m, and 2-m (33-ft, 17-ft, 10-ft, and 7-ft) windows. The observation suggests that 2 m (7 ft) Heterogeneity Log captures optimal heterogeneity in this Mississippian limestones interval. The 1-m window is also used to calculated the Heterogeneity Log. However, the response is similar to the original well-log signature.

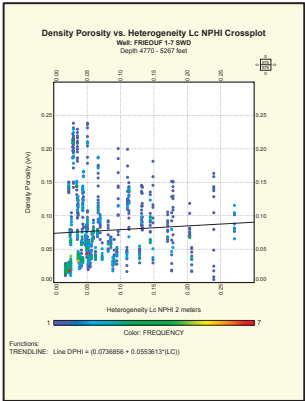
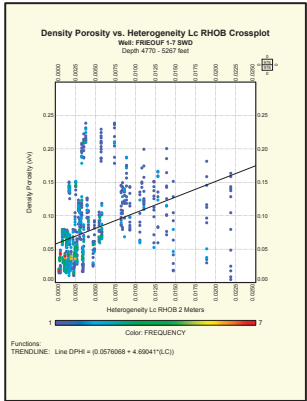


Figure 19. Two (2) crossplots on the left show heterogeneity - Lorenz coefficient of bulk density and neutron porosity versus density derived porosity (DPHI). The petrophysical property derived from the well log shows correlation to the Heterogeneity Logs. There are significant scatter in the cross plots. The multilinear regression suggest that density porosity increases with increasing heterogeneity in bulk density values and neutron porosity heterogeneity values. However, further investigation is needed.

9. Preliminary Observations

1. Based on detailed core description, there are seven (7) lithofacies classes in the Mid-continent Mississippian Limestone in study area. The lithofacies are: 1. brecciated chert; 2. skeletal packstone-grainstone; 3. peloidal mudstone-wackestone; 4. bioturbated peloidal packstone-grainstone; 5. nodular peloidal packstone-grainstone; 6. bedded peloidal packstone-grainstone; and 7. bioturbated mudstone-wackestone.
2. Basic 2-D statistical analysis provides useful information in terms of classifying the electrofacies. However, it has limitations in dealing with multidimensional well-log data and often misclassifies the lithofacies due to significant lithofacies overlapping.
3. The 2-m (7-ft) interval Heterogeneity Log is the best for capturing heterogeneity of petrophysical properties of well-log data.
4. The density porosity derived from bul density shows correlation to the Heterogeneity Log. The density porosity is observed to increase with increasing heterogeneity in bulk density values and neutron porosity heterogeneity values. This relationship may be used for flow-unit characterization; however, further research is required.

10. Future Work

Basic 2-D statistical analysis for petrophysical properties derived from well-log data such as permeability and water saturation will be conducted. In addition, measure of heterogeneity of other well-log data including resistivity, permeability, and water saturation will allow further investigation to reach the research objectives.

Following the measure of heterogeneity of petrophysical properties, relationships of the heterogeneity logs to geological features will be investigated. The investigation will integrate pore types, pore sizes, and mineral compositions derived from multi-mineral analysis, and flow zone indicator (FZI). Once the investigation of Heterogeneity Logs is completed, the next step will be feature selection. In this step, input variables for electrofacies clustering will be selected to provide curves which give the best homogeneous clustering.

The final step will be testing the selected input variables (well-log curves and Heterogeneity Logs) with Artificial-neural network (ANN) and other clustering methods such as Self-organizing Map (SOM) and Multi-resolution Graph-based Clustering (MRGC) for electrofacies classification to explore if the Heterogeneity Log improves electrofacies classification and reservoir characterization in this particular unconventional carbonate reservoir.

References

Birch, C. B., 2015, Reservoir-scale stratigraphy, sedimentology, and porosity characteristics of Mississippian reservoirs, northeastern Anadarko Shelf, Oklahoma, Master's thesis, University of Oklahoma, Norman, Oklahoma. 81 p.

Campbell, J. A., C. J. Mankin, A. B. Schwarzkopf, and J. J. Raymer, 1988, Habitat of petroleum in Permian rocks of the midcontinent region; in, Permian Rocks of the Midcontinent, W. A. Morgan and J. A. Babcock, eds.: Midcontinent Society of Economic Paleontologists and Mineralogists, Special Publication No. 1, p. 13-35

Dutton, S. P., 1984, Fan-Delta Granite Wash of the Texas Panhandle, Oklahoma City Geological Society, vol. Short Course Notes, p. 1-44.

Fitch, P., S. Davies, M. Lovell, T. Pritchard, and C. Sirju, 2010, Heterogeneity in Carbonate Petrophysical Properties: Application to Fluid Flow Units And Sampling Strategies, SPWLA 51st Annual Logging Symposium, Perth, Australia, Society of Petrophysicists and Well-Log Analysts.

Johnson, K. S. and K. V. Luza, 2008, Earth sciences and mineral resources of Oklahoma, Educational Publication 9, Oklahoma Geological Survey, 22 p.

LoCicchio, E., 2012, Wash Play Overview, Anadarko Basin: Stratigraphic Framework and Controls on Pennsylvanian Granite Wash Production, Anadarko Basin, Texas and Oklahoma, AAPG Search and Discovery Article, no. 110163.

McConnell, D. A., 1989, Determination of Offset Across the Northern Margin of the Wichita Uplift, Southwest Oklahoma, Geological Society of America Bulletin, vol. 101, p. 1317-1332.

Mazzullo, S. J., 2011, Mississippian oil reservoirs in the southern midcontinent: New exploration concepts for a mature reservoir objective: Search and Discovery Article 10373.

Nissen, S. E., K. J. Marfurt, and T. R. Carr, 2004, Identifying subtle fracture trends in the Mississippian saline aquifer unit using new 3-D seismic attributes, Kansas Geological Survey Open File Report, no. 56.

Northcutt, R. A. and J. A. Campbell, 1995, Geologic provinces of Oklahoma: Oklahoma Geological Survey Open-File Report 5-95, 1 sheet, scale 1:750,000, 6-page explanation and bibliography.

Acknowledgements

We thank the sponsors of the  
“Mississippi Lime” Consortium at  
the University of Oklahoma

